Electronic Supplementary Information

On the ubiquity of helical a-synuclein tetramers

Liang Xu, Shayon Bhattacharya, & Damien Thompson*

Department of Physics, Bernal Institute, University of Limerick, V94 T9PX, Ireland.

Corresponding Author

*E-mail: Damien.Thompson@ul.ie; Tel: +353 61237734.

Contents

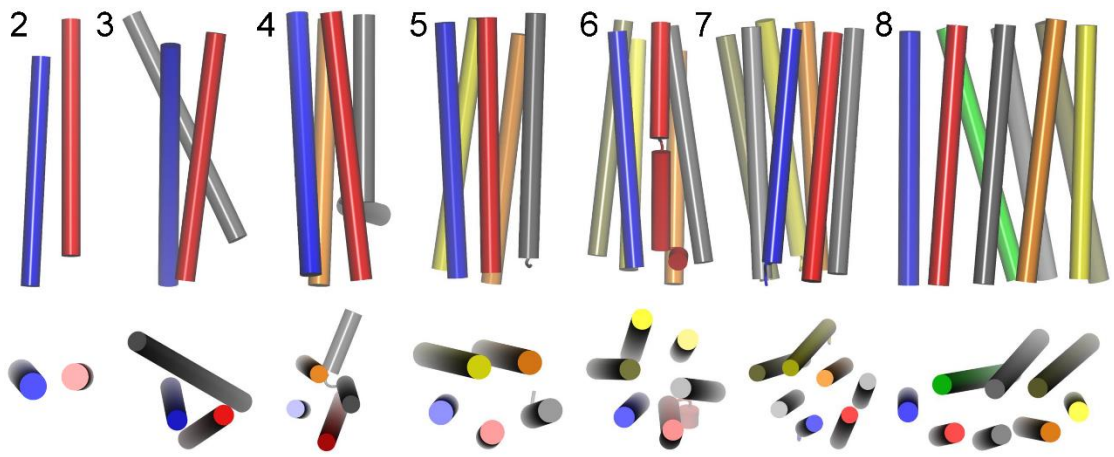

Fig. S1. Side and top views of the final conformations of NAC in mutants. Number 2 to 8 indicates dimer to octamer.

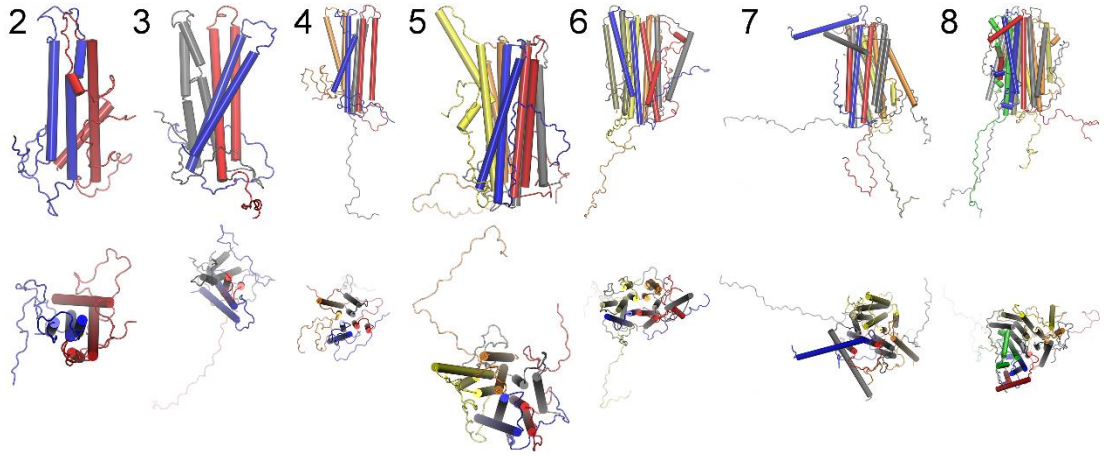

Fig. S2. Side and top views of the final conformations of wild type full-length αS multimers.

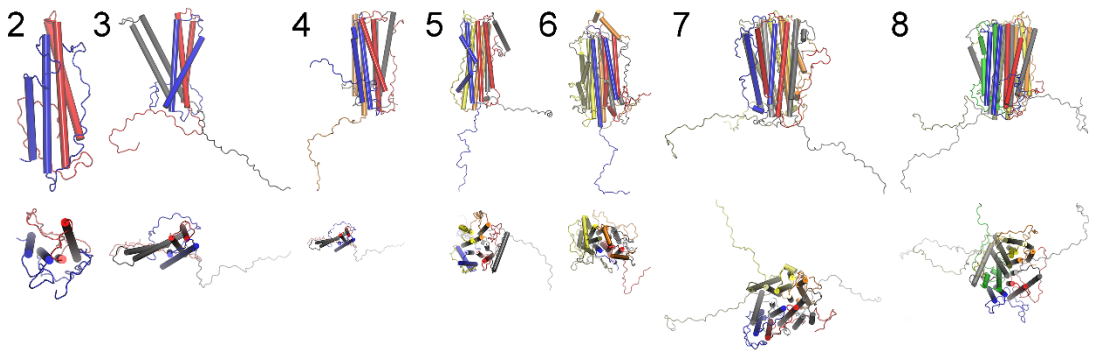

Fig. S3. Side and top views of the final conformations of quadruple mutant (E46K + H50Q + G51D + A53T) full-length αS multimers.

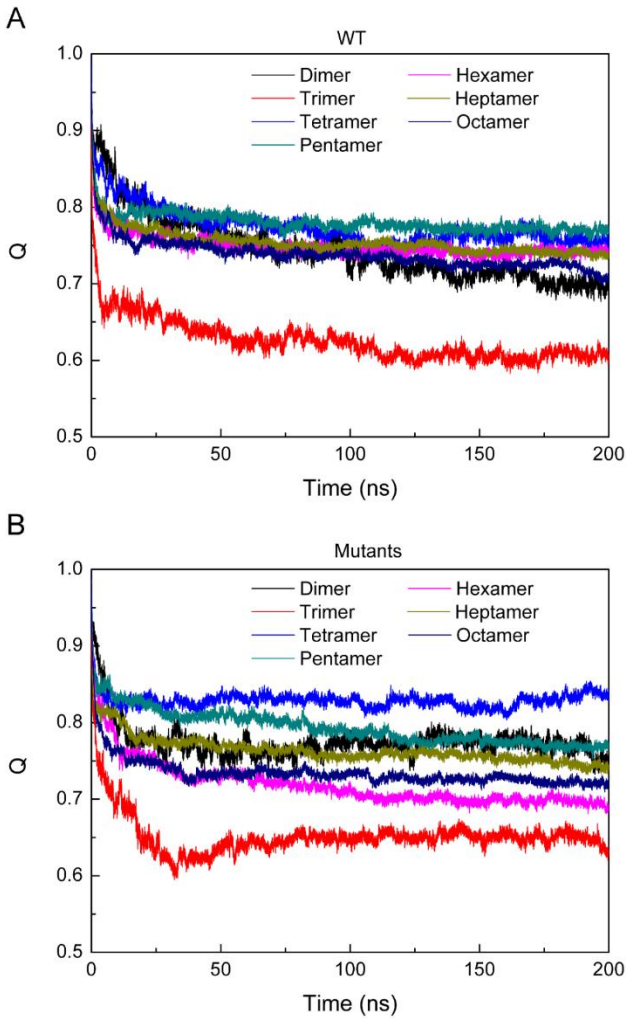

Fig. S4. The fraction of native contacts Q for all αS multimers. The fraction of native contacts was calculated according to the following formula:

$$Q(X) = \frac{1}{N}\sum_{(i,j)} \frac{1}{1+\exp[\beta(r_{ij}(X) - \lambda r_{ij}^{0})]}$$

Heavy atoms i and j in residues θ_i and θ_j are in contact if the distance between them is less than 5.0 Å. r_{ij} (X) is the distance between i and j in conformation X; r^0_{ij} (X) is the distance in the native state (starting conformation). β is a smoothing parameter taken to be 5 $Å^{-1}$ and the factor λ accounts for fluctuations when the contact is formed, taken to be 1.8 for the all-atom model. For more details, see *Proc. Natl. Acad. Sci. U. S. A.*, 2013, 110, 17874.

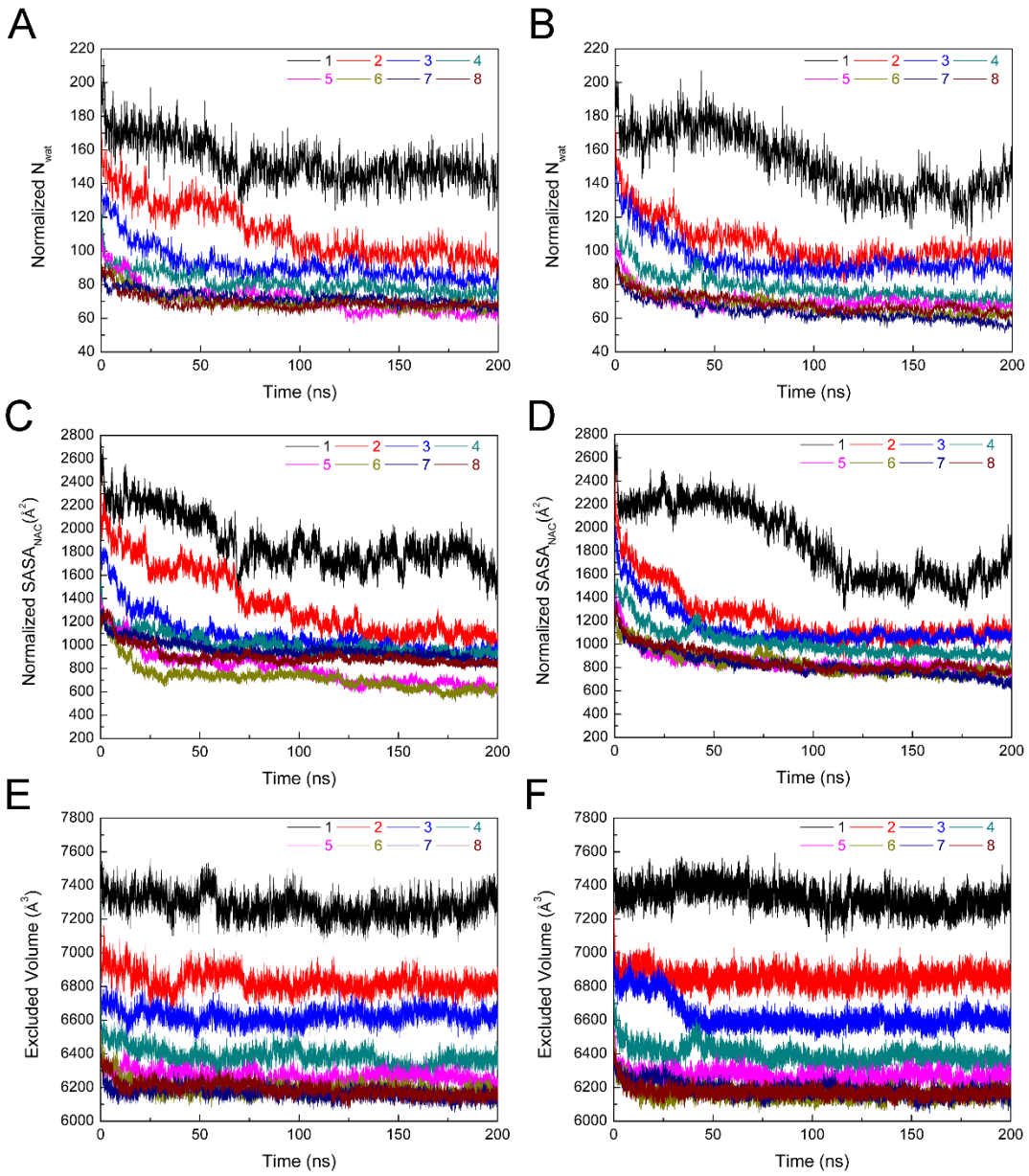

Fig. S5. Normalized number of water molecules within 3.5Å of NAC, solvent accessible surface area (SASA) and water excluded volume for both WT (A, C, and E) and mutated (B, D, and F) helical NAC multimers. The normalized properties were calculated by the total number of water molecules, SASA and excluded volume for each NAC multimer divided by the number of monomers within it.

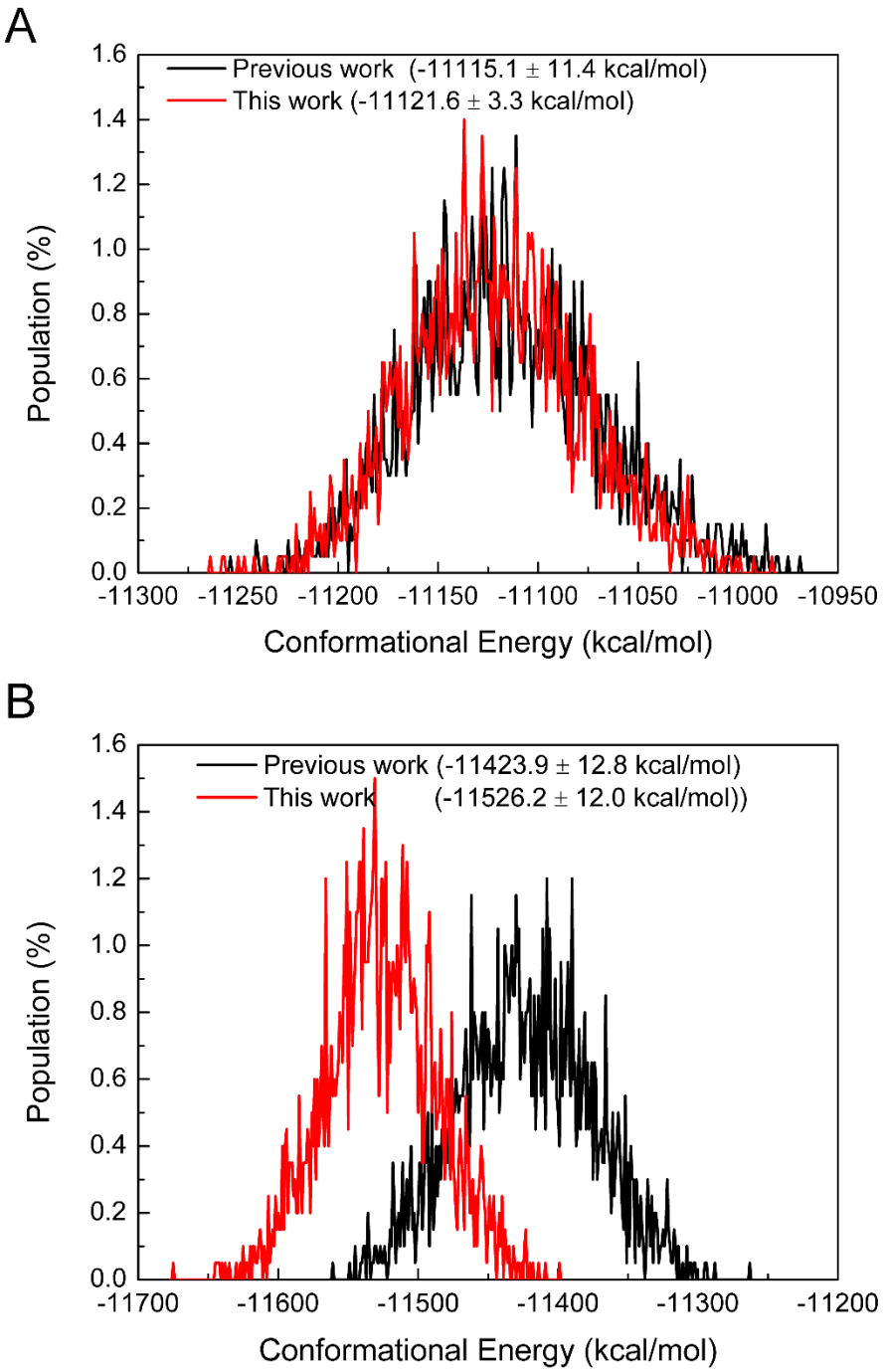

Fig. S6. Comparison of conformational energy between the WT (A) and mutated (B) αS tetramer in our previous work (*Chem. Comm.*, 2018, 54, 8080) and in this work.

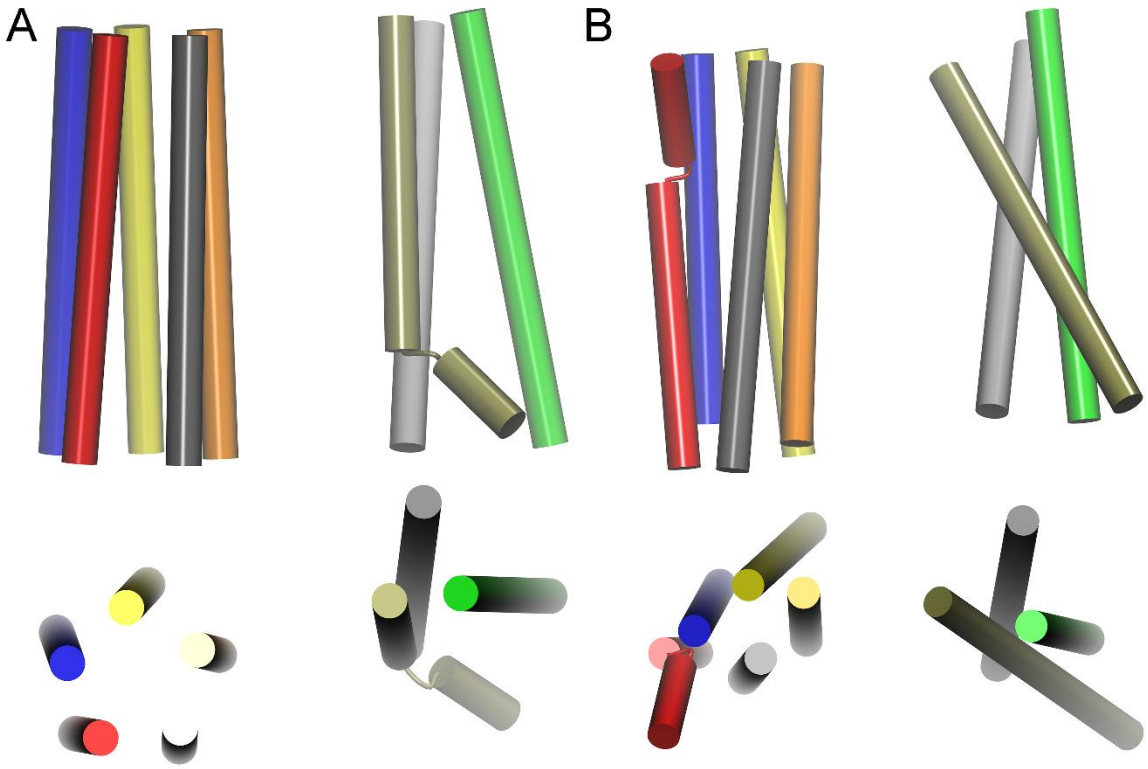

Fig. S7 Designed αS NAC octamer consisting of one NAC pentamer and one trimer with no direct contact between them before (A) and after (B) simulations. The non-NAC pentamer-trimer contacts in the full-length octamer are shown in **Fig. S8.**

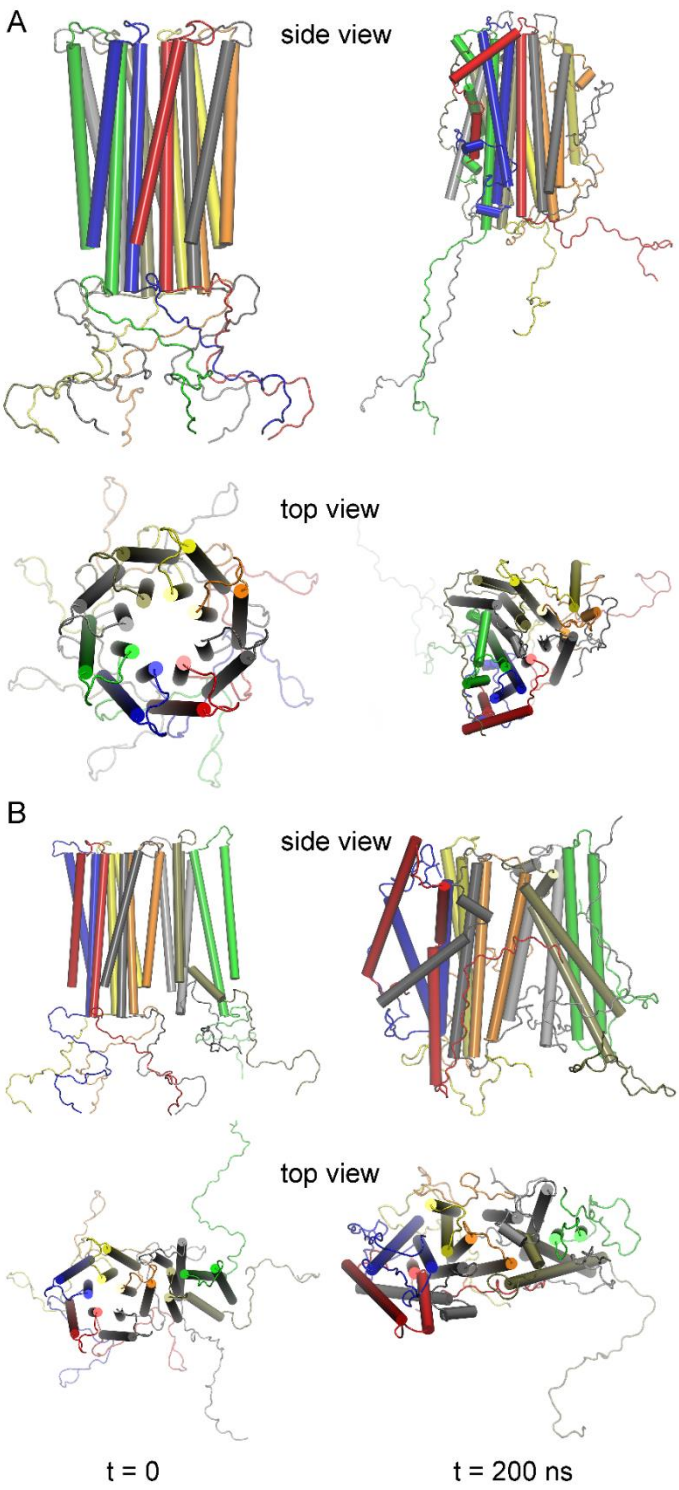

Fig. S8. Conformations of different wild type αS octamers after simulations in both side and top views. Octamer shown in (A) is the same as shown in Fig. 2 and the NAC region is shown by itself for octamer (B) in **Fig. S7**.

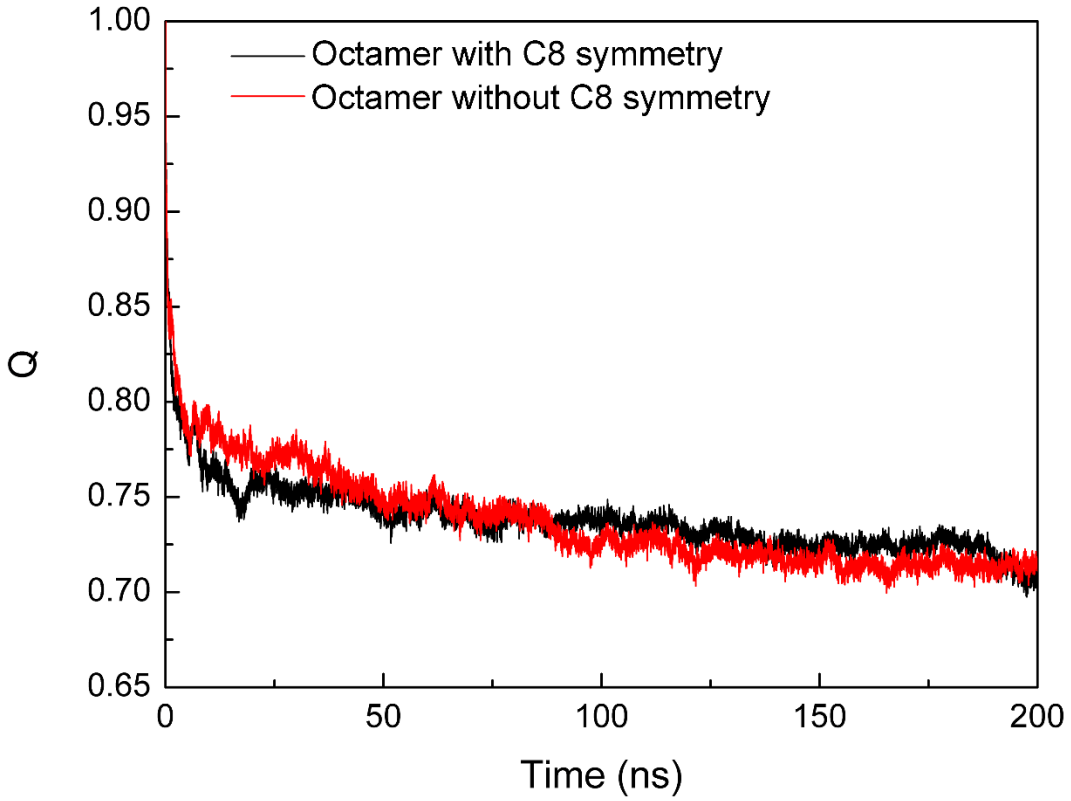

Fig. S9. The fraction of native contacts Q for both αS octamers shown in Fig. S8.

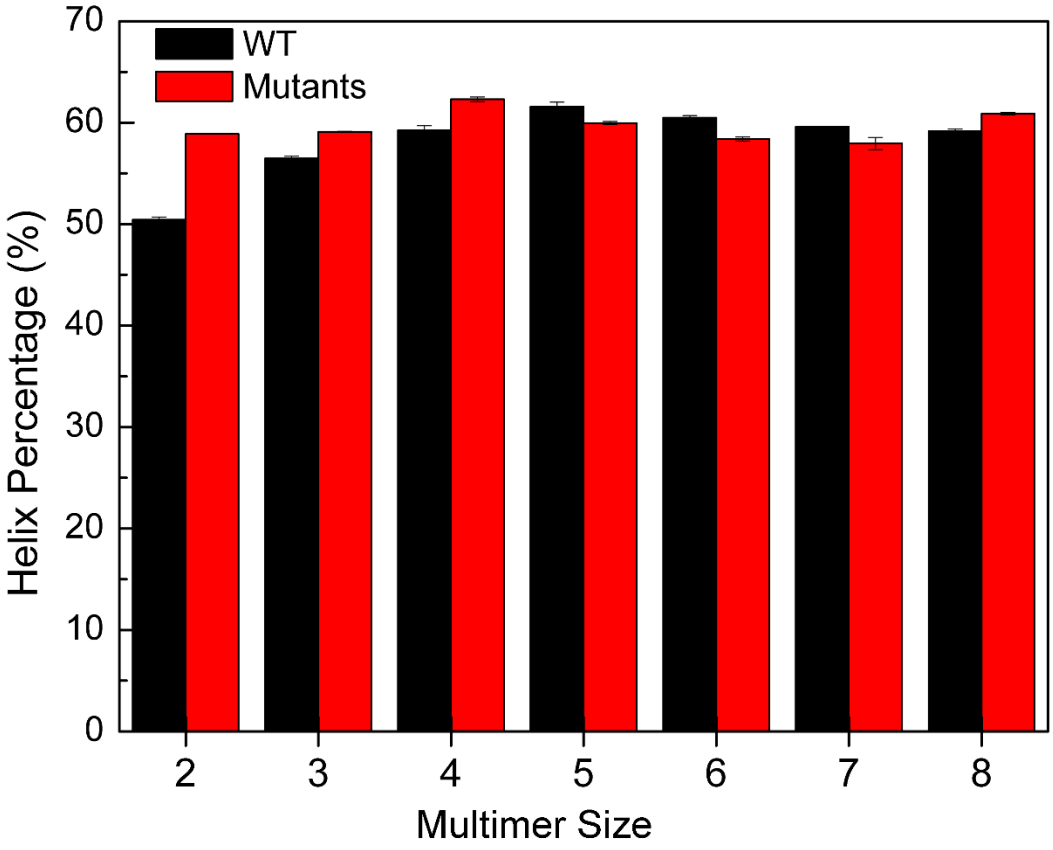

Fig. S10. Percentage helicity for all αS multimers averaged over the last 20-ns of dynamics. The percentage of helix is the sum of α-helix, 3_{10}-helix and π-helix as specified in the Define Secondary Structure of Proteins (DSSP) algorithm. The percentage of helix structure in the initial structure is about 64%.

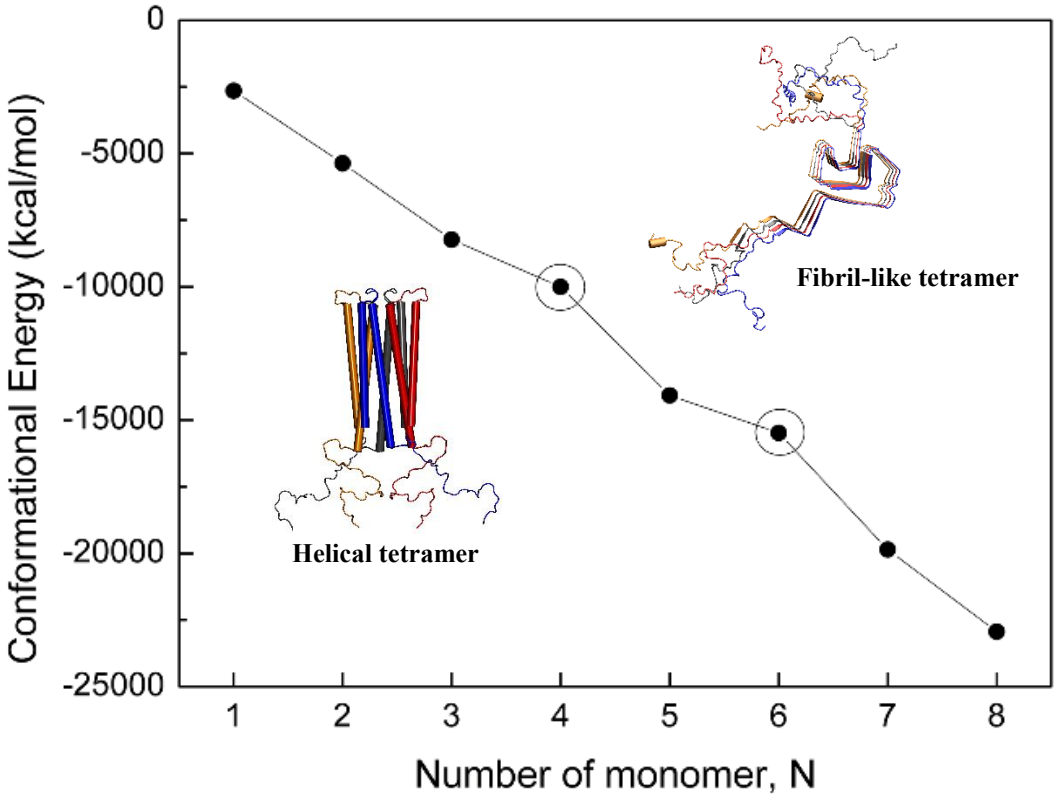

Fig. S11. Relationship between conformational energy and number of monomer units in αS multimers with significant conformational change (tetramer and hexamer in the fibril-like conformation of the Greek Key fold, generated from the fibril PDB ID: 2N0A). Comparison with main text Fig. 3A shows that linear stabilization is established only when no significant conformational change occurs during the assembly of helical α-synuclein.

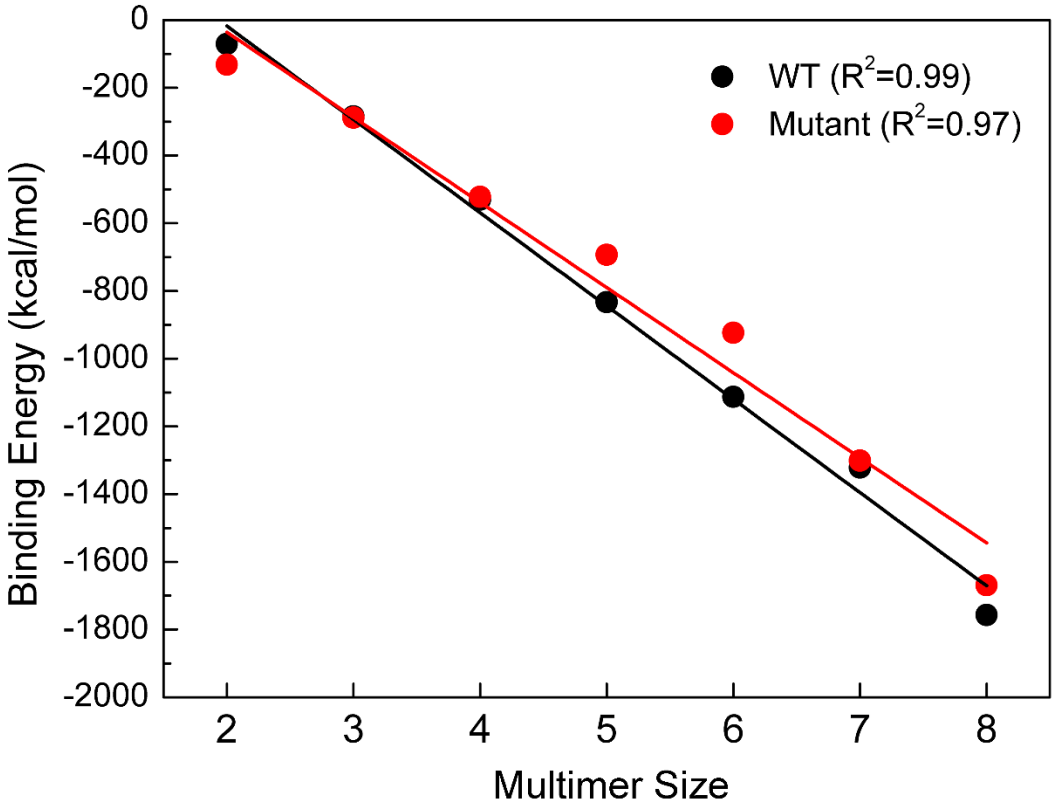

Fig. S12. Binding energy calculated using separate trajectories. The highest binding affinity shown here was the difference in the conformational energy between each multimer and corresponding *n* times of monomers, that is, BE(*n*) = H(*n*) – *n*H(1), where H(*n*) is the conformation energy of the multimer, and H(1) is the conformational energy of free monomer. For calculation details, see **Tables S1 to S3**.

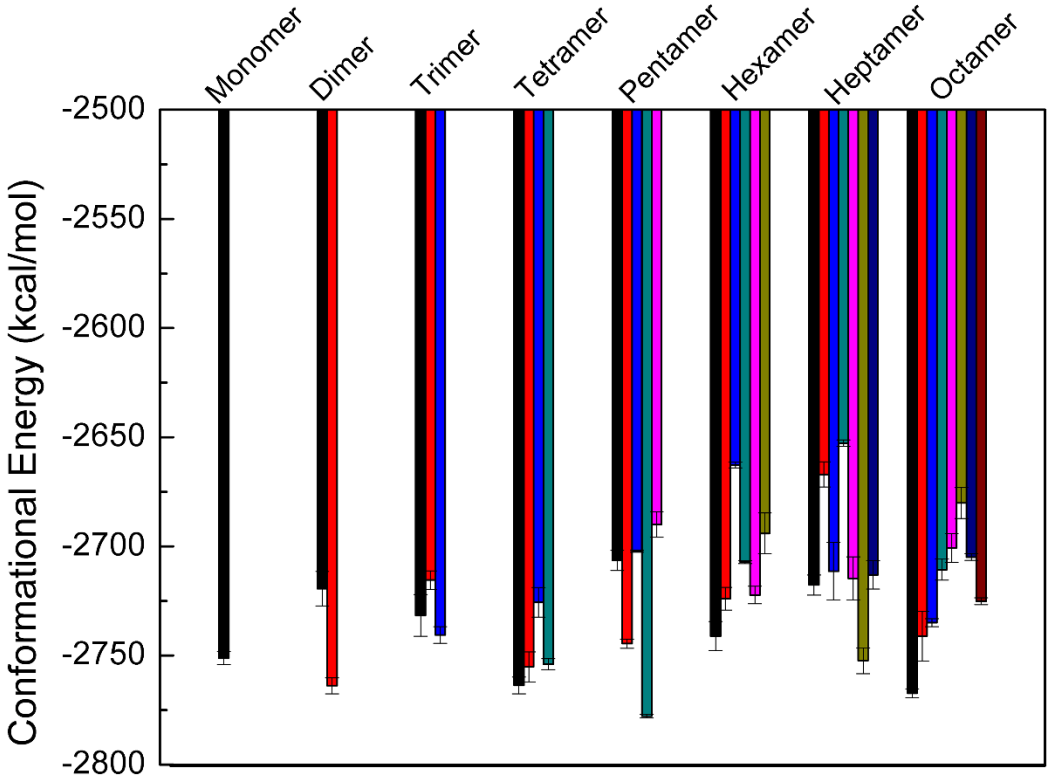

Fig. S13. Conformational energy of individual monomers in different mutants. The conformational energy for the free mutated monomer is shown for comparison.

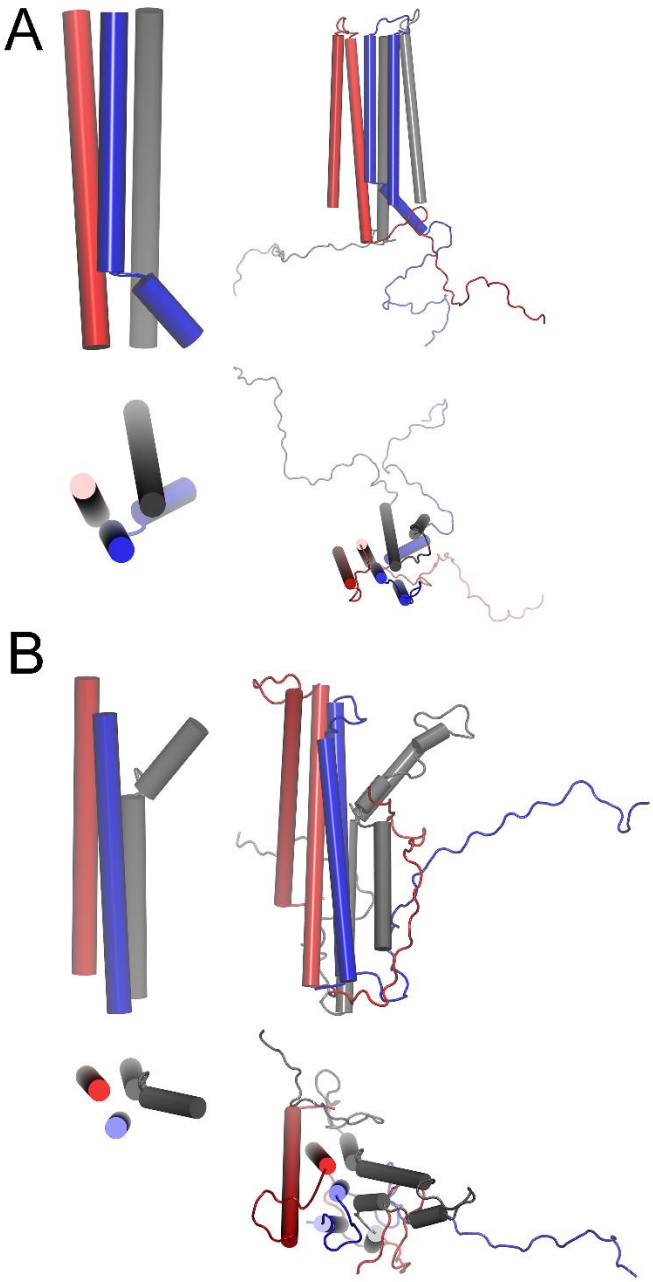

Fig. S14. Helical trimer with its initial conformation taken from our previous tetramer (*Chem. Comm*., 2018, 54, 8080). (A) The initial conformation of the NAC regions and the full-length trimer; (B) Representative conformations for the WT NAC regions and the full-length trimer after 200-ns of molecular dynamics.

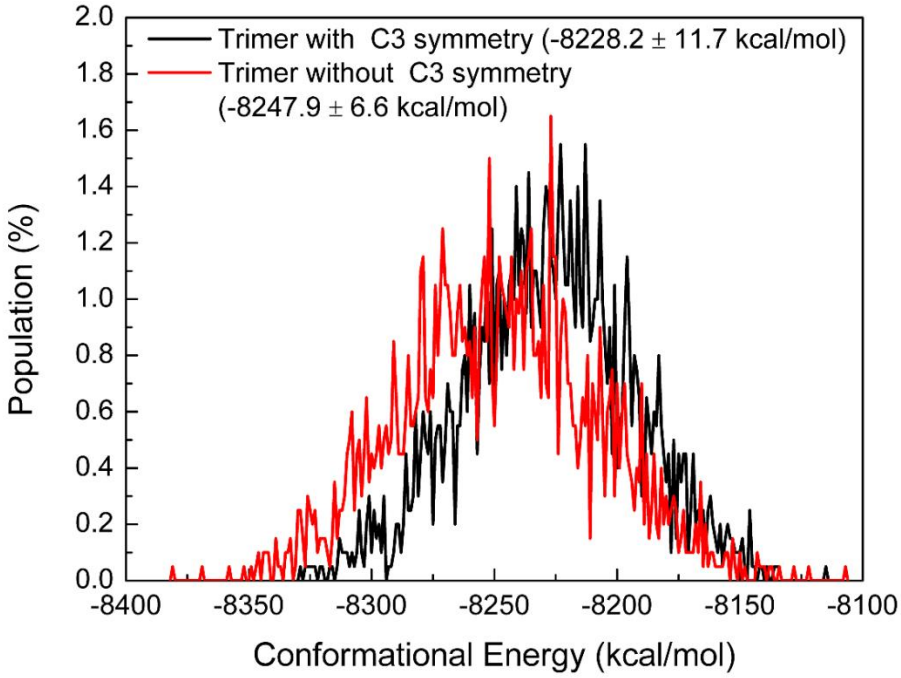

Fig. S15. Statistically distinguishable distributions of conformational energy for different trimers. The trimer with C3 symmetry refers to the trimer shown in **Fig. 2**, and the trimer without C3 symmetry refers to the trimer shown in **Fig. S14**.

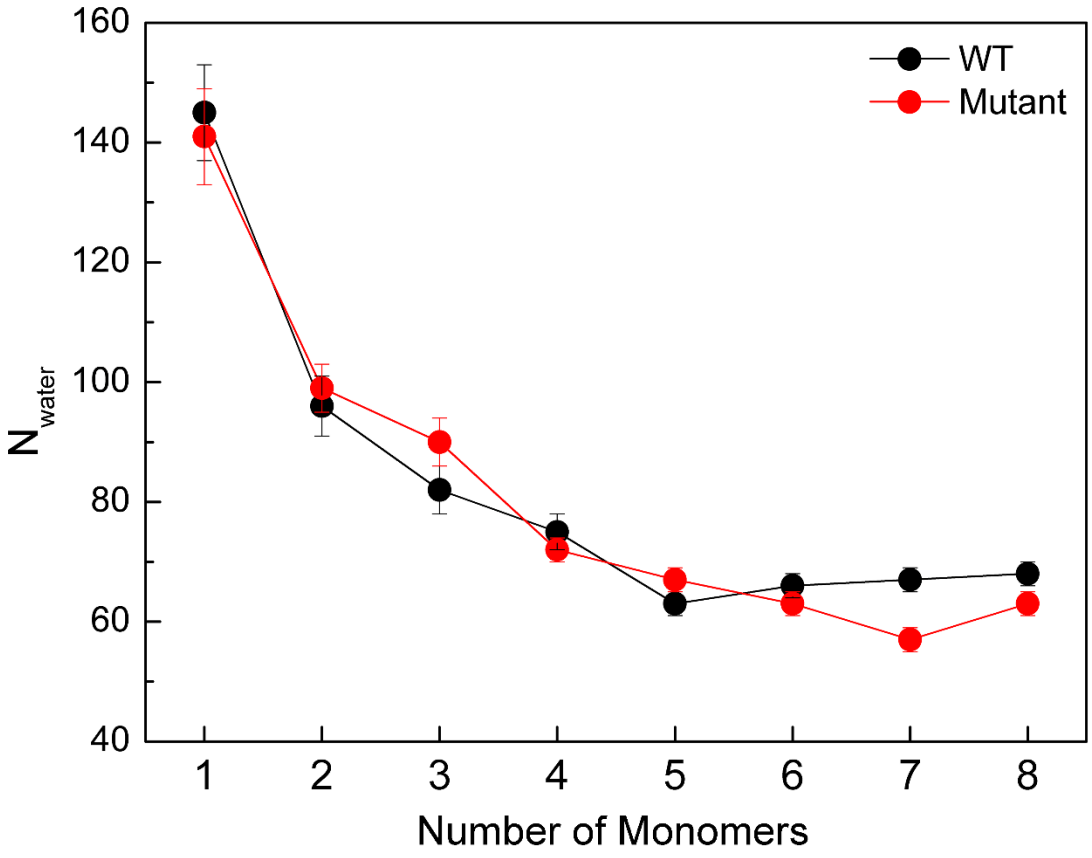

Fig. S16. Normalized number of water molecules within 3.5Å of the NAC region of helical monomer and multimers. The normalized values were calculated by the total number of water molecules near NAC regions divided by the number of monomers within each multimer.

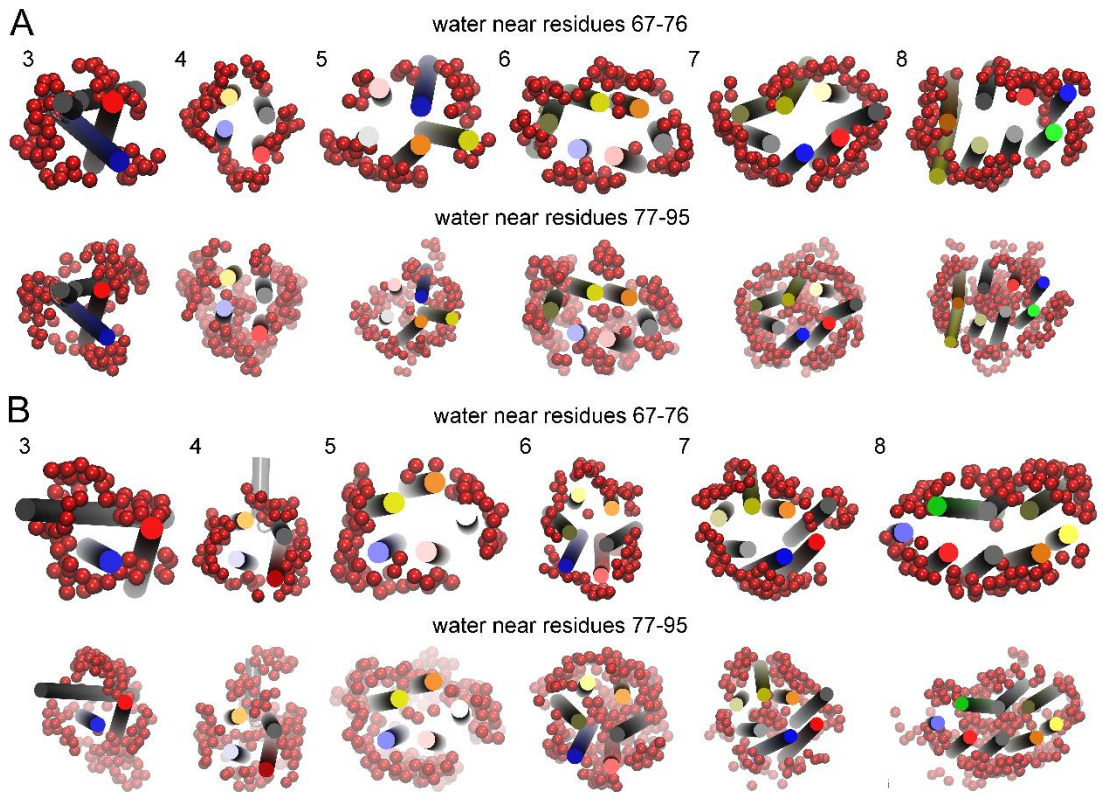

Fig. S17. Representative conformations showing water molecules within 3.5 Å of residues 67–76 and 77–95 of the NAC regions for the WT (A) and mutated (B) helical multimers (trimers to octamers). Water molecules are shown as red balls (oxygen atom).

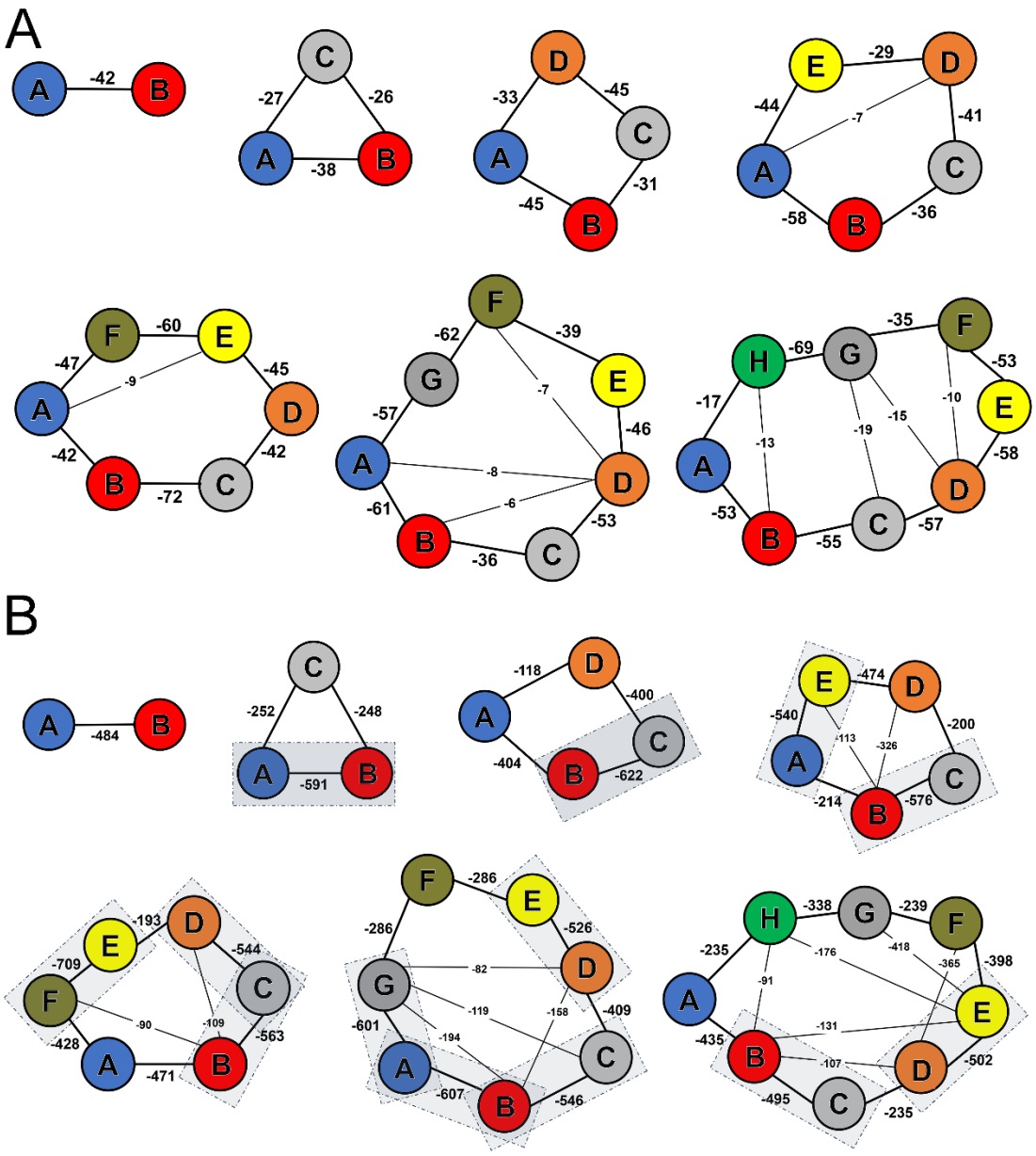

Fig. S18. Pair interaction energies (in kcal/mol) among all NAC regions (A) and all full-length monomers in different mutated multimers. Interactions energies (absolute value) less than 6 kcal/mol in (A) and 82 kcal/mol in (B) were not shown. The pair interactions between monomers stronger or comparable than dimer are highlighted in shaded rectangles (B).

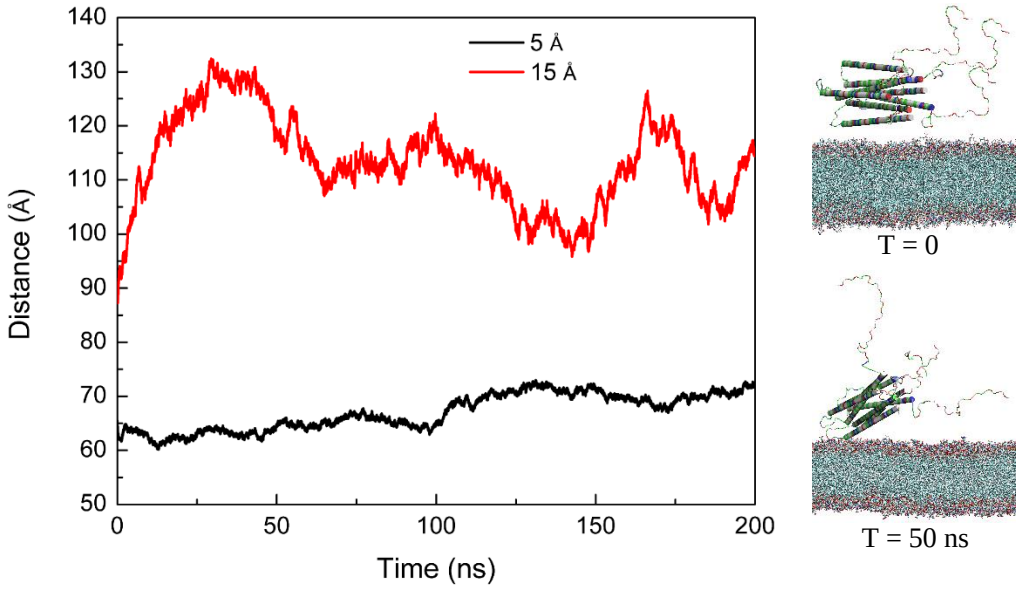

Fig. S19. Time evolution of distance between the center of mass of helical αS tetramer and POPS lipid bilayer over 200-ns MD simulations. Two simulations were performed with initial minimum distances between the tetramer and the membrane set at 5 Å and 15 Å, respectively. Note that no contact was observed throughout the simulation if the initial distance is 15 Å. Weak interactions of the tetramer with the membrane were observed when the initial distance between the tetramer and membrane is 5 Å (starting and final structures are shown in the right hand panel). The tetramer lifts up off the surface of the membrane shifting from a parallel to near perpendicular orientation (see also Fig. 6 in the main text).

Table S1. Conformational energy and average activation energy (in kcal/mol) for all αS multimers.

System		WT		Mutants	
		Conformation	Activation	Conformation	Activation
1	Monomer	-2647.8 (15.7)		-2751.1 (2.9)	
2	Dimer	-5365.9 (9.8)	40.3 (15.1)	-5634.2 (15.0)	9.5 (31.5)
3	Trimer	-8228.2 (11.7)	24.4 (16.4)	-8541.6 (15.1)	21.9 (12.8)
4	Tetramer	-11121.6 (3.3)	7.8 (13.9)	-11526.2 (12.0)	1.5 (16.6)
		-11153.9 (3.5)			
5	Pentamer	-14071.8 (1.4)	23.6 (21.1)	-14448.6 (18.7)	37.4 (21.4)
6	Hexamer	-16999.5 (10.4)	37.8 (27.9)	-17430.1 (27.4)	42.5 (27.6)
		-16934.4 (25.3)			
7	Heptamer	-19855.6 (2.6)	47.6 (19.5)	-20558.8 (11.7)	47.0 (33.6)
8	Octamer	-22939.2 (13.4)	56.8 (27.5)	-23677.8 (2.8)	30.5 (27.3)

Values in bold for systems 4 and 6 are calculated from simulations using a different initial velocity distribution. Activation energies are computed using multiple states each with their own uncertainty and so the overall error estimate can in some cases be higher than the mean.

Table S2. Binding energy of WT αS multimers calculated using separate trajectories. The largest binding affinity for each multimer was shown in **Fig. S12**. "1+1" indicates that the dimer is formed by binding of two monomers; and "1+3" indicates that the tetramer is formed by binding of one monomer and one C3 trimer.

Dimer	**BE (kcal/mol)**
1+1	-70.3
Trimer	**BE**
1+1+1	-284.8
1+2	-214.5
Tetramer	**BE**
1+1+1+1	-530.5
1+1+2	-460.2
1+3	-245.7
2+2	-389.9
Pentamer	**BE**
1+1+1+1+1	-832.9
1+1+1+2	-762.6
1+1+3	-548.1
1+2+2	-692.3
2+3	-477.8
1+4	-302.4

Hexamer	BE
1+1+1+1+1+1	-1112.8
1+1+1+1+2	-1042.5
1+1+1+3	-828.0
1+1+2+2	-972.2
1+2+3	-757.7
1+1+4	-582.3
2+2+2	-901.9
1+5	-279.9
2+4	-512.0
3+3	-543.2

Heptamer	BE
1+1+1+1+1+1+1	-1321.1
1+1+1+1+1+2	-1250.8
1+1+1+1+3	-1036.3
1+1+1+2+2	-1180.5
1+1+2+3	-966.0
1+1+1+4	-790.6
1+2+2+2	-1110.2
1+1+5	-488.2
1+2+4	-720.3

1+3+3	-751.5
2+2+3	-895.7
1+6	-208.3
2+5	-417.9
3+4	-505.8

Octamer	**BE**
1+1+1+1+1+1+1+1	-1756.9
1+1+1+1+1+1+2	-1686.6
1+1+1+1+1+3	-1472.1
1+1+1+1+2+2	-1616.3
1+1+1+2+3	-1401.8
1+1+1+1+4	-1226.4
1+1+2+2+2	-1546.0
1+1+1+5	-924.1
1+1+2+4	-1156.1
1+1+3+3	-1187.3
1+2+2+3	-1331.5
1+1+6	-644.1
1+2+5	-853.8
1+3+4	-941.6
2+2+4	-1085.8
2+3+3	-1117.0

1+7	-435.8
2+6	-573.8
3+5	-639.3
4+4	-695.9

Table S3. Binding energy of mutated αS multimers calculated using separate trajectories. The largest binding affinity for each multimer was shown in **Fig. S12**.

Dimer	**BE (kcal/mol)**
1+1	-132.0
Trimer	**BE**
1+1+1	-288.3
1+2	-156.3
Tetramer	**BE**
1+1+1+1	-521.9
1+1+2	-389.8
1+3	-233.6
2+2	-257.8
Pentamer	**BE**
1+1+1+1+1	-693.1
1+1+1+2	-561.1
1+1+3	-404.8
1+2+2	-429.1
2+3	-272.8
1+4	-171.2

Hexamer	BE
1+1+1+1+1+1	-923.5
1+1+1+1+2	-791.5
1+1+1+3	-635.2
1+1+2+2	-659.5
1+2+3	-503.2
1+1+4	-401.7
2+2+2	-527.4
1+5	-230.4
2+4	-269.6
3+3	-346.9

Heptamer	BE
1+1+1+1+1+1+1	-1301.2
1+1+1+1+1+2	-1169.2
1+1+1+1+3	-1012.9
1+1+1+2+2	-1037.1
1+1+2+3	-880.9
1+1+1+4	-779.3
1+2+2+2	-905.1
1+1+5	-608.1
1+2+4	-647.3

1+3+3	-724.6
2+2+3	-748.8
1+6	-377.7
2+5	-476.1
3+4	-491.0

Octamer	**BE**
1+1+1+1+1+1+1+1	-1669.0
1+1+1+1+1+1+2	-1537.0
1+1+1+1+1+3	-1380.7
1+1+1+1+2+2	-1405.0
1+1+1+2+3	-1248.7
1+1+1+1+4	-1147.2
1+1+2+2+2	-1273.0
1+1+1+5	-975.9
1+1+2+4	-1015.2
1+1+3+3	-1092.4
1+2+2+3	-1116.7
1+1+6	-745.5
1+2+5	-843.9
1+3+4	-858.9
2+2+4	-883.1
2+3+3	-960.4

1+7	-367.9
2+6	-613.5
3+5	-687.6
4+4	-625.3

References

1. Xu, L.; Bhattacharya, S.; Thompson, D. Re-designing the α-synuclein tetramer. *Chem. Commun.* **2018,** *54*, 8080-8083.
2. Pierce, B.; Tong, W.; Weng, Z. M-ZDOCK: a grid-based approach for Cn symmetric multimer docking. *Bioinformatics* **2005,** *21*, 1472-8.
3. Huang, J.; Rauscher, S.; Nawrocki, G.; Ran, T.; Feig, M.; de Groot, B. L.; Grubmüller, H.; MacKerell, A. D. CHARMM36m: an improved force field for folded and intrinsically disordered proteins. *Nat. Methods* **2016,** *14*, 71-73.
4. Abraham, M. J.; Murtola, T.; Schulz, R.; Páll, S.; Smith, J. C.; Hess, B.; Lindahl, E. GROMACS: High performance molecular simulations through multi-level parallelism from laptops to supercomputers. *SoftwareX* **2015,** *1-2*, 19-25.
5. Bussi, G.; Donadio, D.; Parrinello, M. Canonical sampling through velocity rescaling. *J. Chem. Phys.* **2007,** *126*, 014101.
6. Parrinello, M.; Rahman, A. Polymorphic transitions in single crystals: A new molecular dynamics method. *J. App. Phys.* **1981,** *52*, 7182-7190.
7. Brooks, B. R.; Bruccoleri, R. E.; Olafson, B. D.; States, D. J.; Swaminathan, S.; Karplus, M. CHARMM: A program for macromolecular energy, minimization, and dynamics calculations. *J. Comput. Chem.* **1983,** *4*, 187-217.
8. Lee, M. S.; Salsbury, F. R.; Brooks, C. L. Novel generalized Born methods. *J. Chem. Phys.* **2002,** *116*, 10606-10614.
9. Lee, M. S.; Feig, M.; Salsbury, F. R.; Brooks, C. L. New analytic approximation to the standard molecular volume definition and its application to generalized Born calculations. *J. Comput. Chem.* **2003,** *24*, 1348-1356.
10. Feig, M.; Onufriev, A.; Lee, M. S.; Im, W.; Case, D. A.; Brooks, C. L. Performance comparison of generalized born and Poisson methods in the calculation of electrostatic solvation energies for protein structures. *J. Comput. Chem.* **2004,** *25*, 265-284.